

Influence of Calcium(II) and Chloride on the Oxidative Reactivity of a Manganese(II) Complex of a Cross-Bridged Cyclen Ligand

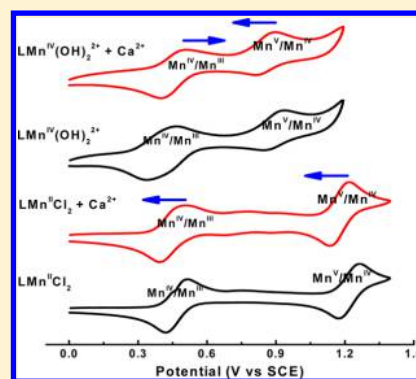
Zhan Zhang,[†] Katherine L. Coats,[‡] Zhuqi Chen,[†] Timothy J. Hubin,^{*,‡} and Guochuan Yin^{*,†}

[†]Key Laboratory for Large-Format Battery Materials and System, Ministry of Education, School of Chemistry and Chemical Engineering, Hubei Key Laboratory of Material Chemistry and Service Failure, Huazhong University of Science and Technology, Wuhan 430074, P. R. China

[‡]Department of Chemistry and Physics, Southwestern Oklahoma State University, 100 Campus Drive, Weatherford, Oklahoma 73096, United States

S Supporting Information

ABSTRACT: Available data from different laboratories have confirmed that both Ca^{2+} and Cl^- are crucial for water oxidation in Photosystem II. However, their roles are still elusive. Using a manganese(II) complex having a cross-bridged cyclen ligand as a model, the influence of Ca^{2+} on the oxidative reactivity of the manganese(II) complex and its corresponding manganese(IV) analogue were investigated. It has been found that adding Ca^{2+} can significantly improve the oxygenation efficiency of the manganese(II) complex in sulfide oxidation and further accelerate the oxidation of sulfoxide to sulfone. Similar improvements have also been observed for Mg^{2+} , Sr^{2+} , and Ba^{2+} . A new monomeric manganese(IV) complex having two *cis*-hydroxide ligands has also been isolated through oxidation of the corresponding manganese(II) complex with H_2O_2 in the presence of NH_4PF_6 . This rare *cis*-dihydroxomanganese(IV) species has been well characterized by X-ray crystallography, electrochemistry, electron paramagnetic resonance, and UV–vis spectroscopy. Notably, using the manganese(IV) complex as a catalyst demonstrates higher activity than the corresponding manganese(II) complex, and adding Ca^{2+} further improves its catalytic efficiency. However, adding Cl^- decreases its catalytic activity. In electrochemical studies of manganese(IV) complexes with no chloride ligand present, adding Ca^{2+} positively shifted the redox potential of the $\text{Mn}^{\text{IV}}/\text{Mn}^{\text{III}}$ couple but negatively shifted its $\text{Mn}^{\text{V}}/\text{Mn}^{\text{IV}}$ couple. In the manganese(II) complex having a chloride ligand, adding Ca^{2+} shifted both the $\text{Mn}^{\text{IV}}/\text{Mn}^{\text{III}}$ and $\text{Mn}^{\text{V}}/\text{Mn}^{\text{IV}}$ couples in the negative direction. The revealed oxidative reactivity and redox properties of the manganese species affected by Ca^{2+} and Cl^- may provide new clues to understanding their roles in the water oxidation process of Photosystem II.



INTRODUCTION

Oxygen evolution through water oxidation in Photosystem II (PSII) is a crucial process in nature. The available data have clearly demonstrated that the oxygen evolution center (OEC) is comprised of a Mn_4CaO_5 core in which the manganese atoms directly participate in water oxidation through a $\text{S}_0\text{--S}_4$ cycle.¹ During the $\text{S}_0\text{--S}_4$ cycle, the oxidation states of manganese in the Mn_4CaO_5 cluster change from 2+ to 4+, or even a proposed 5+, in a stepwise manner as the electron-transfer processes proceed. Many synthetic models have been developed to help understand the physicochemical properties of the Mn_4CaO_5 core, and additional small-molecule redox catalysts have been explored for catalytic water oxidation to generate oxygen.^{2,3} As part of the increased understanding of the manganese-catalyzed water oxidation in PSII, both calcium(II) and chloride have been recognized to play significant roles in the catalytic cycle, even though their exact roles are still unclear.

For calcium(II), it has been generally believed that it is essential for the S state to develop beyond S_2 .⁴ Moreover, van Gorkom further suspected that Ca^{2+} is also required in all of the S-state transitions.⁵ Particularly, with extensive electrochemical

studies on a series of MMn_3O_4 ($\text{M} = \text{Ca}^{2+}$, Sr^{2+} , Zn^{2+} , etc.) complexes, Agapie et al. proposed that Ca^{2+} may regulate the redox potentials of manganese ions in the catalytic cycle.⁶ Pecoraro and Brudvig proposed that Ca^{2+} is possibly involved in the O–O bond formation during oxygen evolution through attack on the terminal $\text{Mn}^{\text{V}}=\text{O}$ functional group by a Ca^{2+}OH or $\text{Ca}^{2+}\text{OH}_2$; Brudvig et al. further suggests that Ca^{2+} serves as a Lewis acid, which activates the substrate water molecule or hydroxide anion to facilitate its nucleophilic attack on $\text{Mn}^{\text{V}}=\text{O}$.^{1b,7} Notably, on the basis of the resolved X-ray structure, Ferreira et al. proposed that the monomeric manganese appendage is the site of the water oxidation event (Figure 1).⁸ If the $\text{Mn}^{\text{V}}=\text{O}$ site proposed by Pecoraro and Brudvig for O–O bond formation, the monomeric manganese appendage, is correct, investigating the redox behaviors of OEC in water oxidation with monomeric manganese models becomes particularly valuable.

Received: June 11, 2014

Published: November 6, 2014



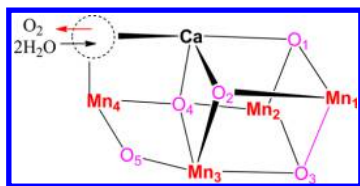


Figure 1. Structure of the OEC based on a recent X-ray structure. One potential site for H₂O binding and O₂ formation is indicated.

In theoretical studies by quantum mechanical/molecular mechanical calculations, it has been proposed that Ca²⁺ is bound to the Mn₄ cluster by a μ -O or μ -OH bridge, and the Ca²⁺ activated water (Ca²⁺OH₂) attacks the oxyl radical, Mn^{IV}O•, rather than Mn^V=O, to generate the O–O bond before oxygen evolution.^{1a,9} Alternatively, Siegbahn et al. suggest that oxyl radicals react with Mn–O–Mn bridges instead of reacting with terminal Ca²⁺OH₂ to form the O–O bond.¹⁰ Compared with relatively extensive studies and an increasing understanding of Ca²⁺ in water oxidation, the role of chloride is even more elusive, and the precise binding site of Cl[−] is still controversial.¹¹ These limited studies have proposed that Cl[−] may affect the electron-transfer events in the S-state transitions by modulating the redox potential of the manganese ions or neutralizing and stabilizing the accumulated positive charge in the S states.¹² Batista et al. have also proposed that the role(s) of Cl[−] are possibly related to proton transfer in the catalytic cycle.¹³ Notably, Yocum et al. suggested that Cl[−] is required for the S-state transitions from S₂ to S₃ and from S₃ to S₀,^{12b} where Ca²⁺ is essential as well, implying that Ca²⁺ and Cl[−] may synergistically participate in these S-state transitions.

Although versatile protocols have been applied to deplete Ca²⁺ or Cl[−] for investigating their roles in the actual oxygen evolution process in natural systems, similar studies using synthetic models to investigate how Ca²⁺ and Cl[−] affect the redox chemistry of the manganese ion are very limited. Borovik et al. have reported that the presence of Ca²⁺ can accelerate oxygen activation by their manganese(II) and iron(II) complexes,¹⁴ and Agapie et al. revealed that the redox-inactive metal ions, as Lewis acids, can affect the electrochemical properties of their [MMn₃O₄] cubane clusters, which are structurally related to the Mn₄CaO₅ core in the OEC.⁶

Like redox-inactive Ca²⁺'s role in oxygen evolution, many other redox-inactive metal ions may also play significant roles in heterogeneous oxidations, like stabilizing the redox catalysts or modulating their reactivity.¹⁵ Addressing how these redox-inactive metal ions affect the reactivity of an active metal ion has recently attracted significant attention in the biomimetic community. The available results from different models have revealed that adding Lewis acids like Sc³⁺, Al³⁺, or even BF₃ or Brønsted acid (H⁺) can accelerate active iron oxo (Fe^{IV}=O) or manganese oxo (Mn^{IV}=O, Mn^V=O, or MnO₄[−]) mediated electron transfer, oxygenation, or hydrogen abstraction rates.^{16–19} The acceleration effects are related to binding of the Lewis acid to the redox metal oxo (Mⁿ⁺=O) or its protonation by Brønsted acid, which leads to positively shifted redox potentials. These findings have greatly promoted the understanding of how the redox-inactive metal ions affect the oxidative properties of an active metal ion. However, up to now, there has been no detailed example to probe the influence of Ca²⁺ on the redox chemistry of the manganese ion in a catalytic process.^{19h} In this work, we report an example of how Ca²⁺ and Cl[−] affect the catalytic oxidation properties and the

redox potentials of the manganese ion using a monomeric manganese model having a cross-bridged cyclen ligand.

EXPERIMENTAL SECTION

Mn^{II}(Me₂Bcyclen)Cl₂, Mn^{II}(Me₂EBC)Cl₂, Mn^{II}(TPA)Cl₂, and Mn^{II}(BPMEN)Cl₂ [Me₂Bcyclen = 4,10-dimethyl-1,4,7,10-tetraazabicyclo[5.5.2]tetradecane; EBC = 4,11-dimethyl-1,4,8,11-tetraazabicyclo[6.6.2]hexadecane; TPA = tris(2-pyridylmethyl)amine; BPMEN = *N,N'*-dimethyl-*N,N'*-bis(2-pyridylmethyl)ethane-1,2-diamine] were synthesized according to literature procedures,^{20–22} and the structures of these ligands are shown in Figure 2. All other

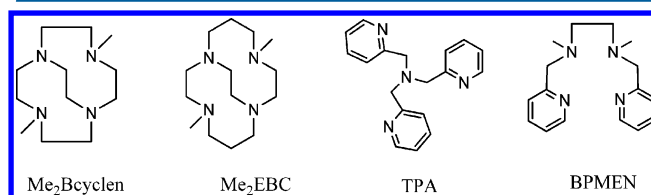


Figure 2. Structures of the ligands used in this study.

chemical reagents are commercially available. Electrochemical studies were performed on a CS Corrtest electrochemical workstation equipped with glassy carbon as both the working and counter electrodes and saturated calomel as the reference electrode, and the redox potentials were measured under argon in dry acetonitrile with 0.1 M tetrabutylammonium perchlorate as the supporting electrolyte. Kinetic data were collected on an Analytikjena specord 205 UV–vis spectrometer, and gas chromatography–mass spectrometry (GC–MS) analysis was performed on an Agilent 7890A/5975C spectrometer. Electron paramagnetic resonance (EPR) experiments were conducted at 130 K on a Bruker A200 spectrometer.

Synthesis of [Mn^{IV}(Me₂Bcyclen)(OH)₂](PF₆)₂. A 2 mL aqueous solution containing 0.10 g (0.28 mmol) of Mn^{II}(Me₂Bcyclen)Cl₂ and 0.093 g (0.56 mmol) of NH₄PF₆ was prepared. A total of 1 mL of 30% H₂O₂ was added stepwise with stirring to the prepared solution over a period of 2 h, which generates a blue-purple solution immediately. The resulting solution was stirred until bubbles were no longer formed (about 1 h). During this period, a blue-purple precipitate was gradually generated, which was filtered on a glass frit and washed with H₂O. The product was collected and dried overnight under reduced pressure at room temperature. A total of 0.074 g of crude product was obtained as a blue-purple powder. Yield: 43%. To purify the crude product, it was completely dissolved in 2 mL of H₂O to generate a saturated aqueous solution. Then, 1 mL of an aqueous solution saturated with 50 mg of NH₄PF₆ was added stepwise to the solution with stirring, which gradually led to the formation of a blue-purple precipitate. The precipitate was filtered and dried under reduced pressure at room temperature to obtain the purified blue-purple powder product. Yield: 60% (from the crude product). Anal. Calcd for MnC₁₂H₂₈N₄O₃P₂F₁₂: C, 23.81; H, 4.66; N, 9.26. Found: C, 23.80; H, 4.66; N, 9.03. The X-ray-quality crystal of [Mn^{IV}(Me₂Bcyclen)(OH)₂](PF₆)₂ was obtained by diffusion of ether into an acetone solution containing [Mn^{IV}(Me₂Bcyclen)(OH)₂](PF₆)₂ at 258 K.

Crystal Structure Analysis. A blue-purple prism-shaped crystal of dimensions 0.66 × 0.50 × 0.40 mm was selected for X-ray structure analysis. Intensity data for this compound were collected on a Rigaku Mercury CCD diffractometer at 293(2) K using graphite-monochromated Mo K α radiation (λ = 0.71073 Å) with a ω -scan method. The centrosymmetric monoclinic space group P2₁/n was determined by systematic absences and statistical tests and verified by subsequent refinement. The structure was solved by direct methods and refined by full-matrix least-squares methods on F². One target molecule was cocrystallized with 1 equiv of acetone. Both counteranions, PF₆[−], are disordered. The hydrogen atoms H(1)O and H(2)O, which are bound to the oxygen atoms O(1) and O(2), are located in the difference Fourier synthesis and were refined semifreely with the help of a distance restraint, while constraining their U values to 1.2 times the

$U(\text{eq})$ values of corresponding oxygen atoms. All of the other hydrogen atoms are placed in calculated positions and refined by using a riding model.

Catalytic Sulfide Oxidation by Manganese(II) Complexes with Lewis Acid. In 5 mL of dry acetonitrile containing 0.1 M thioanisole, 0.33 mM manganese(II) complex, and 0.33 mM Lewis acid, for example, $\text{Ca}(\text{OTf})_2$, 0.2 mL of 30% H_2O_2 was added to initialize the reaction. The reaction mixture was stirred in a H_2O bath at 303 K for 6 h, and the product analysis was performed by GC using the internal standard method. Control experiments using the manganese(II) complex or Lewis acid alone as the catalyst were carried out in parallel.

Catalytic Methyl Phenyl Sulfoxide Oxidation by Manganese(II) Complexes with Ca^{2+} . In 5 mL of dry acetonitrile containing 0.1 M methyl phenyl sulfoxide, 0.33 mM manganese(II) complex, and 0.33 mM $\text{Ca}(\text{OTf})_2$, 0.2 mL of 30% H_2O_2 was added to initialize the reaction. The reaction mixture was stirred in an ice H_2O bath (273 K) for 2 h, and product analysis was performed by GC using the internal standard method. Control experiments using the manganese(II) complex alone as the catalyst were carried out in parallel.

Catalytic Sulfide Oxidation by Manganese(IV) Complexes with Ca^{2+} . In 5 mL of dry acetonitrile containing 0.1 M thioanisole, a 0.33 mM manganese(IV) complex, and 0.33 mM $\text{Ca}(\text{OTf})_2$, 0.2 mL of 30% H_2O_2 was added to initialize the reaction. The reaction mixture was stirred in an ice H_2O bath (273 K) for 4 h, and product analysis was performed by GC using the internal standard method. Control experiments using the manganese(IV) complex alone as the catalyst were carried out in parallel.

Stoichiometric Oxygenation by the Manganese(IV) Complexes with Ca^{2+} . In 5 mL of a dry acetonitrile solvent, 0.01 mmol of the manganese(IV) complex, 0.01 mmol of $\text{Ca}(\text{OTf})_2$, and 0.01 mmol of triphenylphosphine were added. The resulting reaction mixture was stirred in a H_2O bath at 298 K for 4 h, and product analysis was performed by GC using the internal standard method. Control experiment using the manganese(IV) complex alone was carried out in parallel.

Catalytic Hydrogen Abstraction by Manganese(II) Complexes with Ca^{2+} . In 5 mL of dry acetonitrile containing 0.1 M 1,4-cyclohexadiene, a 0.33 mM manganese(II) complex, 0.33 mM $\text{Ca}(\text{OTf})_2$, and 0.2 mL of 30% H_2O_2 were added. The resulting reaction mixture was stirred in a H_2O bath at 303 K for 4 h, and product analysis was conducted by GC using the internal standard method. Control experiments using the manganese(II) complex or $\text{Ca}(\text{OTf})_2$ alone as the catalyst were carried out in parallel.

RESULTS AND DISCUSSION

Catalytic Sulfide Oxidation by Manganese(II) Complexes with Ca^{2+} . Because it has been hypothesized that the water oxidation event may happen on the monomeric manganese appendage of Mn_4CaO_5 in the OEC and Ca^{2+} is possibly involved in the O–O bond formation for oxygen evolution,^{7,8} investigating how Ca^{2+} and Cl^- affect the redox behavior of monomeric manganese model complexes becomes informative to understanding water oxidation in the OEC. Here, using a manganese model having a cross-bridged cyclen ligand, $\text{Mn}^{\text{II}}(\text{Me}_2\text{Bcyclen})\text{Cl}_2$, the influence of Ca^{2+} and its analogues like Mg^{2+} , Sr^{2+} , or Ba^{2+} on the oxidative reactivity of manganese was investigated using H_2O_2 as the terminal oxidant, and the results are summarized in Table 1. Although understanding the effects of Ca^{2+} and Cl^- on the oxidation of sulfide by a mononuclear manganese catalyst cannot provide equal insight into OEC chemistry, the obtained knowledge about how Ca^{2+} and Cl^- affect the redox behavior of a manganese ion may aid the eventual understanding of their roles in OEC chemistry.

In the control experiment without both manganese complexes and Lewis acid, oxidation of thioanisole at 303 K

Table 1. Catalytic Sulfide Oxidation by Manganese(II) Complexes with Lewis Acid^a

catalyst	additive	conversion (%)	yield of monoxide (%)	yield of dioxide (%)
		12.0	7.2	4.5
Mn^{II}		65.9	32.6	25.9
Mn^{II}	CaCl_2	87.6	39.4	36.7
Mn^{II}	$\text{Mg}(\text{OTf})_2$	90.6 (17.8)	37.8 (5.1)	38.7 (4.4)
Mn^{II}	$\text{Ca}(\text{OTf})_2$	91.4 (18.9)	44.1 (8.1)	37.1 (5.3)
Mn^{II}	$\text{Sr}(\text{NO}_3)_2$	98.0 (18.6)	34.4 (7.9)	49.2 (3.7)
Mn^{II}	$\text{Ba}(\text{OTf})_2$	97.8 (16.7)	31.6 (6.1)	50.8 (3.6)

^aConditions: solvent, acetonitrile 5 mL; thioanisole, 0.1 M; manganese(II) catalyst, 0.33 mM; Lewis acid, 0.33 mM; H_2O_2 , 0.2 mL; 303 K, 6 h. The data in parentheses represent the control experiment without the manganese(II) catalyst.

with H_2O_2 provides only 7.2% sulfoxide and 4.5% sulfone as products in 6 h, and the conversion of thioanisole is only 12.0%. The $\text{Mn}^{\text{II}}(\text{Me}_2\text{Bcyclen})\text{Cl}_2$ catalyst alone is active, giving 65.9% conversion of sulfide with 32.6% and 25.9% yield of sulfoxide and sulfone, respectively. Adding 1 equiv of $\text{Ca}(\text{OTf})_2$ to the $\text{Mn}^{\text{II}}(\text{Me}_2\text{Bcyclen})\text{Cl}_2$ catalyst substantially improved its oxygenation activity, providing 91.4% conversion and 44.1% yield of sulfoxide with 37.1% of sulfone products. Using $\text{Ca}(\text{OTf})_2$ alone as the catalyst yields results similar to those in the control experiment. In another test, adding CaCl_2 in place of $\text{Ca}(\text{OTf})_2$ to the $\text{Mn}^{\text{II}}(\text{Me}_2\text{Bcyclen})\text{Cl}_2$ complex generates oxygenation improvements similar to those of $\text{Ca}(\text{OTf})_2$, indicating that it is Ca^{2+} , rather than OTf^- , that accelerates the oxidation reaction. In GC analysis of the products, some trace peaks were observed in addition to the dominant sulfoxide and sulfone products, which can be attributed to the formation of C–S cleavage products (vide infra).

Mg^{2+} generates an acceleration effect similar as to that of Ca^{2+} , while Sr^{2+} and Ba^{2+} are slightly more active than Ca^{2+} . For example, in the presence of $\text{Sr}(\text{NO}_3)_2$, thioanisole can be almost completely converted, which provides 34.4% yield of sulfoxide and 49.2% yield of sulfone, while $\text{Sr}(\text{NO}_3)_2$ alone is also inactive like those in the control experiment. Because $\text{Sr}(\text{OTf})_2$ is not commercially available, in situ generated $\text{Sr}(\text{OTf})_2$ by reaction of SrCl_2 with $\text{Ag}(\text{OTf})$ (after filtering AgCl precipitate) gives similar results, that is, 34.5% yield of sulfoxide and 47.1% yield of sulfone with 98.1% conversion, supporting the theory that the acceleration effect is directly related to Sr^{2+} . Notably, adding Mg^{2+} , Ca^{2+} , Sr^{2+} , or Ba^{2+} not only accelerates $\text{Mn}^{\text{II}}(\text{Me}_2\text{Bcyclen})\text{Cl}_2$ -catalyzed sulfide oxidation but also substantially improves sulfone formation. For example, the $\text{Mn}^{\text{II}}(\text{Me}_2\text{Bcyclen})\text{Cl}_2$ catalyst alone gives only 25.9% yield of the sulfone product under the described conditions, while adding 1 equiv of Ca^{2+} improves the yield up to 37.1% and Sr^{2+} gives an even higher 49.2% yield of sulfone. In complementary experiments, it was found that adding Mg^{2+} , Ca^{2+} , Sr^{2+} , or Ba^{2+} to sulfide, sulfoxide, or sulfone does not shift the UV–vis spectra, indicating that no interaction exists between the added Lewis acid and substrate or products.

Interestingly, increasing the ratio of Ca^{2+} to manganese(II) catalyst further improves the oxidation of thioanisole and greatly increases the yield of sulfone. In the presence of 4 equiv of Ca^{2+} , the conversion of thioanisole reaches 98.5%, and the yield of sulfone increases to 67.7%, with only 24.0% yield of sulfoxide [see Table S1 in the Supporting Information (SI) for details]. The catalytic kinetics further confirms that adding Ca^{2+}

can accelerate the $\text{Mn}^{\text{II}}(\text{Me}_2\text{Bcyclen})\text{Cl}_2$ -catalyzed thioanisole oxidation rate. As shown in Figure 3, in each data point compared with using the manganese(II) catalyst alone, the presence of Ca^{2+} can accelerate the substrate conversion and product formations simultaneously.

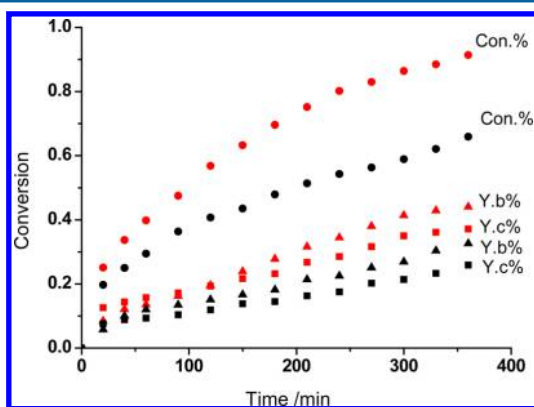


Figure 3. Oxygenation kinetics of thioanisole by the manganese(II) complex in the presence (red shapes) and absence (black shapes) of Ca^{2+} . Conditions: solvent, acetonitrile 5 mL; thioanisole, 0.1 M; manganese(II) catalyst, 0.33 mM; $\text{Ca}(\text{OTf})_2$, 0.33 mM; H_2O_2 , 0.2 mL; 303 K. Y.b% represents the yield of sulfoxide, and Y.c% represents the yield of sulfone.

Adding Ca^{2+} may accelerate not only thioanisole oxidation but also oxidation of sulfoxide to sulfone, which is indicated in Table 1. Notably, oxidation of sulfoxide is faster than that of sulfide. To determine the acceleration effect of Ca^{2+} , oxidations were performed under ice H_2O conditions to slow the oxidation rate. When using methyl phenyl sulfoxide in place of thioanisole as the substrate, after 2 h of reaction in ice H_2O (273 K), the $\text{Mn}^{\text{II}}(\text{Me}_2\text{Bcyclen})\text{Cl}_2$ catalyst alone provides 54.7% conversion of sulfoxide with 44.3% yield of sulfone. Adding 1 equiv of Ca^{2+} to the catalyst achieved 64.9% conversion of substrate with 51.5% yield of sulfone (see Table S2 in the SI for details). Obviously, although Ca^{2+} and its analogues are inactive for sulfide oxidation, they can substantially accelerate manganese(II)-catalyzed oxidation.

In the literature, it has been reported that Sr^{2+} is the only other redox-inactive metal ion that can functionally, but partially, replace Ca^{2+} in PSII.²³ Here, the metal ions Mg^{2+} , Sr^{2+} , and Ba^{2+} all generated acceleration effects similar to that of Ca^{2+} . Possibly, in PSII, the protein environment surrounding the OEC prohibits other metal ions from playing a role identical with that of Ca^{2+} , although active Sr^{2+} can recover up to 40% function of Ca^{2+} .^{23a,b} However, with our small-molecule catalyst, all of the redox-inactive metal ions may freely interact with the manganese catalyst in bulk solvent. As a result, all of these metal ions have demonstrated similar acceleration effects. Certainly, the oxygenation mechanism of sulfide demonstrated here is very different from oxygen evolution in PSII, which requires stepwise electron transfer in the O–O bond formation through the S_0 – S_4 cycle. Therefore, a direct comparison between the results obtained here with those in PSII is not possible.

Oxidations of different sulfides were also investigated, and the results are listed in Table 2. Under the identical conditions of thioanisole oxidation by $\text{Mn}^{\text{II}}(\text{Me}_2\text{Bcyclen})\text{Cl}_2$ in the presence of 1 equiv of Ca^{2+} , diphenyl sulfide oxidation provides 88.2% conversion with 47.9% yield of diphenyl sulfoxide and

Table 2. Oxidations of Different Sulfides by Manganese(II) Complexes with $\text{Ca}(\text{OTf})_2$ ^a

substrate	conversion (%)	yield of monoxide (%)	yield of dioxide (%)
thioanisole	91.4 (65.9)	44.1 (32.6)	37.1 (25.9)
diphenyl sulfide	88.2 (58.7)	47.9 (37.9)	26.7 (10.3)
benzyl phenyl sulfide	93.1 (82.2)	21.7 (24.3)	50.4 (30.6)

^aConditions: solvent, acetonitrile 5 mL; sulfide, 0.1 M; manganese(II) catalyst, 0.33 mM; $\text{Ca}(\text{OTf})_2$, 0.33 mM; H_2O_2 , 0.2 mL; 303 K, 6 h. The data in parentheses represent the control experiment with manganese(II) catalyst alone.

26.7% yield of diphenyl sulfone. Benzyl phenyl sulfide gives 93.1% conversion with 21.7% sulfoxide and 50.4% sulfone. Significantly, in each case, using the manganese(II) catalyst alone yielded less sulfoxide and sulfone products than obtained by adding Ca^{2+} , as shown in the parentheses of Table 2. In addition to being a common substrate in sulfide oxidation, benzyl phenyl sulfide is a unique substrate that can serve as a probe to provide extra mechanistic information. In sulfide oxidation, the reaction may proceed by concerted oxygen transfer or electron transfer. In the case of electron transfer, the sulfide radical cation intermediate, $\text{R-S}^{\bullet+}\text{-R}$, will be generated from the substrate, and its instability leads to rearrangement and formation of various C–S cleavage products.²⁴ Here, through GC–MS analysis, the C–S cleavage products, including phenol, benzaldehyde, benzyl alcohol, benzyl phenyl ether, 1,2-diphenylethane, etc., have been identified in benzyl phenyl sulfide oxidation (see Figure S1 in the SI for details). This result indicates the occurrence of an electron-transfer process in its oxidation.

Experiments for Catalytic Hydrogen Abstraction by Manganese(II) Complexes with Ca^{2+} . In complementary experiments, the influence of Ca^{2+} on catalytic hydrogen abstraction reactions of manganese(II) complexes was also investigated, although it is not directly related to oxygen evolution in PSII. To simplify the reaction, 1,4-cyclohexadiene was employed as the substrate because it would provide solely benzene as the product. Without Ca^{2+} , using H_2O_2 as the oxidant in acetonitrile, the manganese(II) complex as the catalyst provides 17.8% yield of benzene with 18.5% conversion. Adding Ca^{2+} slightly improves the hydrogen abstraction efficiency, giving 23.4% benzene with 34.4% conversion of 1,4-cyclohexadiene.

Synthesis and Characterization of the Manganese(IV) Complex. In the catalytic oxidation cycle, we suspected that a manganese intermediate at high oxidation state would be generated in situ under oxidative conditions. Particularly, in PSII, it has been suggested that Ca^{2+} would affect the S-state transitions beyond the S_2 state, in which the oxidation state of all of the manganese atoms in the Mn_4CaO_5 cluster will be 4+, or even higher.^{1,4} Thus, to address how Ca^{2+} affects the oxidative reactivity of these intermediates at high oxidation state, it is essential to isolate the active manganese intermediates in this study. Previously, a manganese(IV) complex having a cross-bridged cyclam ligand, $\text{Mn}^{\text{IV}}(\text{Me}_2\text{EBC})(\text{OH})_2(\text{PF}_6)_2$ (Me_2EBC = 4,11-dimethyl-1,4,8,11-tetraazabicyclo[6.6.2]hexadecane), was synthesized using H_2O_2 .²⁵ Following a similar preparation, its analogue, $\text{Mn}^{\text{IV}}(\text{Me}_2\text{Bcyclen})(\text{OH})_2(\text{PF}_6)_2$, was also successfully synthesized by oxidation of $\text{Mn}^{\text{II}}(\text{Me}_2\text{Bcyclen})\text{Cl}_2$ with aqueous H_2O_2 in the presence of NH_4PF_6 . A crystal suitable for X-ray analysis

has also been isolated by diffusion of ether into an acetone solution. The crystal data and structure refinement of the manganese(IV) complex are listed in Table 3, with the selected bond distances (Å) and angles (deg) listed in Table 4 and the cation unit of the manganese(IV) complex shown in Figure 4.

Table 3. Crystal Data and Structure Refinement for $\text{Mn}^{\text{IV}}(\text{Me}_2\text{Bcyclen})(\text{OH})_2(\text{PF}_6)_2 \cdot \text{CH}_3\text{COCH}_3$

empirical formula	$\text{C}_{15}\text{H}_{34}\text{F}_{12}\text{MnN}_4\text{O}_3\text{P}_2$
fw	663.34
temperature (K)	293(2)
wavelength (Å)	0.71073
cryst syst	monoclinic
space group	$P2_1/n$
unit cell dimens	
<i>a</i> (Å)	13.392(3)
<i>b</i> (Å)	10.614(2)
<i>c</i> (Å)	19.239(4)
α (deg)	90
β (deg)	90.29(3)
γ (deg)	90
volume (Å ³)	2734.7(9)
Z	4
density (calcd) (Mg m ⁻³)	1.611
abs coeff (mm ⁻¹)	0.706
<i>F</i> (000)	1356
cryst color and habit	black block
cryst size (mm ³)	0.66 × 0.50 × 0.40
θ range for data collection (deg)	3.23–27.46
index ranges	−17 ≤ <i>h</i> ≤ 17, −10 ≤ <i>k</i> ≤ 13, −18 ≤ <i>l</i> ≤ 24
reflns collected	12688
indep reflns	6176 [<i>R</i> (int) = 0.0382]
completeness to θ = 27.46° (%)	98.8
abs corrn	semiempirical from equivalents
max and min transmn	1.0000 and 0.7685
refinement method	full-matrix least squares on <i>F</i> ²
data/restraints/param	6176/675/454
GOF on <i>F</i> ²	1.119
final <i>R</i> indices [<i>I</i> > 2σ(<i>I</i>)]	<i>R</i> 1 = 0.0782, <i>wR</i> 2 = 0.1587
<i>R</i> indices (all data)	<i>R</i> 1 = 0.1274, <i>wR</i> 2 = 0.1837
largest diff peak and hole (e Å ⁻³)	0.397 and −0.271

Selected bond lengths and angles for $\text{Mn}^{\text{IV}}(\text{Me}_2\text{Bcyclen})(\text{OH})_2^{2+}$ are summarized in Table 4. The Mn–O lengths in $\text{Mn}^{\text{IV}}(\text{Me}_2\text{Bcyclen})(\text{OH})_2^{2+}$ are 1.801(3) and 1.799(3) Å, clearly establishing the presence of $\text{Mn}^{\text{IV}}\text{--OH}$ moieties. These bond lengths are slightly shorter than the octahedral 1.830(4) Å $\text{Mn}^{\text{IV}}\text{--OH}$ bond in trinuclear $[\text{Mn}_3\text{O}_4(\text{OH})(\text{bepa})_3]_3$ [bepa = *N,N*-bis(2-pyridylmethyl)ethylamine]²⁶ and also shorter than the monoclinic 1.811(2) Å $\text{Mn}^{\text{IV}}\text{--O}$ bond in $\text{Mn}^{\text{IV}}(\text{Me}_2\text{EBC})(\text{OH})_2^{2+}$, in which hydrogen-bond formation was found between the hydrogen atom in the hydroxo moiety and water molecule.²⁵ In the previously characterized $\text{Mn}^{\text{IV}}(\text{Me}_2\text{EBC})(\text{OH})_2(\text{PF}_6)_2$ complex, the X-ray-quality crystal was obtained from H_2O under reduced pressure, while here the crystal of $\text{Mn}^{\text{IV}}(\text{Me}_2\text{Bcyclen})(\text{OH})_2(\text{PF}_6)_2$ was obtained by diffusion of ether into its acetone solution; thus, there is no water molecule in its crystal structure. The Mn–O lengths in $\text{Mn}^{\text{IV}}(\text{Me}_2\text{Bcyclen})(\text{OH})_2^{2+}$ are also slightly shorter than that [1.807(3) Å] of $\text{Mn}^{\text{III}}\text{--O}$ in $[\text{Mn}^{\text{III}}(\text{PYS})(\text{OH})]^{2+}$, which is expected from the ionic radii $\text{Mn}^{4+} < \text{Mn}^{3+}$.²⁷ However, the

Table 4. Selected Bond Distances (Å) and Angles (deg) of the $\text{Mn}^{\text{IV}}(\text{Me}_2\text{Bcyclen})(\text{OH})_2^{2+}$ Cation

Mn–O	O(1)–Mn(1)	1.801(3)
	O(2)–Mn(1)	1.799(3)
Mn–N	N(1)–Mn(1)	2.047(4)
	N(5)–Mn(1)	2.028(3)
	N(8)–Mn(1)	2.047(4)
	N(12)–Mn(1)	2.042(4)
N–Mn–N	N(5)–Mn(1)–N(12)	84.5(2)
	N(5)–Mn(1)–N(8)	82.4(2)
	N(12)–Mn(1)–N(8)	85.1(2)
	N(5)–Mn(1)–N(1)	85.5(2)
	N(12)–Mn(1)–N(1)	82.0(2)
	N(8)–Mn(1)–N(1)	163.1(2)
O–Mn–O	O(2)–Mn(1)–O(1)	97.6(2)
O–Mn–N	O(2)–Mn(1)–N(5)	173.8(2)
	O(1)–Mn(1)–N(5)	88.6(2)
	O(2)–Mn(1)–N(12)	89.3(2)
	O(1)–Mn(1)–N(12)	173.0(2)
	O(2)–Mn(1)–N(8)	97.2(2)
	O(2)–Mn(1)–N(1)	93.6(2)
	O(1)–Mn(1)–N(8)	93.4(2)
	O(1)–Mn(1)–N(1)	98.0(2)

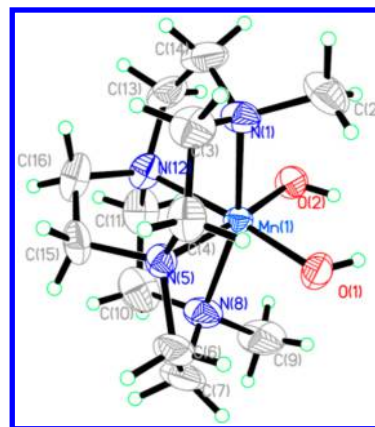


Figure 4. Structure of $\text{Mn}^{\text{IV}}(\text{Me}_2\text{Bcyclen})(\text{OH})_2^{2+}$. Ellipsoids are drawn at the 30% probability level.

manganese(III) ion is in a rhombic octahedral environment and may experience pseudo-Jahn–Teller distortion. Moreover, the $\text{Mn}^{\text{IV}}\text{--O}$ lengths in $\text{Mn}^{\text{IV}}(\text{Me}_2\text{Bcyclen})(\text{OH})_2^{2+}$ are also shorter than 1.873(2) Å of the $\text{Mn}^{\text{III}}\text{--O}$ bond in five-coordinated $[\text{Mn}^{\text{III}}(\text{H3L})(\text{OH})]$ ($\text{H6L} = [\text{tris}[(N'\text{-tert-butylur-} \text{eayl})\text{-}N\text{-ethyl}]]\text{amine}$) in which the OH ligand is hydrogen-bonded to a urea nitrogen atom of the H3L ligand.²⁸ The average length of the Mn–N bonds is 2.041 Å in $\text{Mn}^{\text{IV}}(\text{Me}_2\text{Bcyclen})(\text{OH})_2^{2+}$ [2.047(4), 2.028(3), 2.047(4), and 2.042(4) Å, respectively], a value clearly shorter than those observed in $\text{Mn}^{\text{IV}}(\text{Me}_2\text{EBC})(\text{OH})_2^{2+}$ [2.110(3) and 2.090(2) Å]. This difference is attributed to a more compact coordination environment encompassed by the $\text{Me}_2\text{Bcyclen}$ ligand than the Me_2EBC ligand. The ease with which the cross-bridged tetraazamacrocycle encompasses the metal varies with the ligand size and is further demonstrated by the *axial* and *equatorial* N–Mn–N bond angles. The $N_{\text{ax}}\text{--Mn--}N_{\text{ax}}$ angles decrease in the order of 175.7(1)° for $\text{Mn}^{\text{IV}}(\text{Me}_2\text{EBC})(\text{OH})_2^{2+}$ and 163.1(2)° for $\text{Mn}^{\text{IV}}(\text{Me}_2\text{Bcyclen})(\text{OH})_2^{2+}$, and the $N_{\text{ax}}\text{--Mn--}N_{\text{eq}}$ bond angles decrease in the same order: 91.0(1)° for $\text{Mn}^{\text{IV}}(\text{Me}_2\text{EBC})(\text{OH})_2^{2+}$ and 82.0(2)° for $\text{Mn}^{\text{IV}}(\text{Me}_2\text{Bcyclen})\text{--}$

(OH)₂²⁺. Thus, the manganese ion in Mn^{IV}(Me₂Bcyclen)-(OH)₂²⁺ is less encompassed by the cross-bridged macrocycle and more exposed to a potential solvent, oxidant, or substrate in comparison with Mn^{IV}(Me₂EBC)(OH)₂²⁺.

Electronic Structure. The cyclic voltammogram of the Mn^{IV}(Me₂Bcyclen)(OH)₂(PF₆)₂ complex is shown in Figure 5,

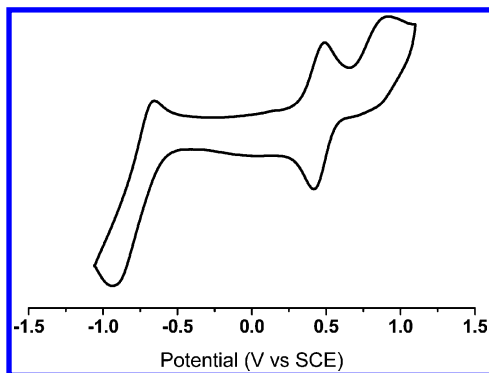


Figure 5. Cyclic voltammogram for [Mn^{IV}(Me₂Bcyclen)(OH)₂](PF₆)₂ in dry acetonitrile at 298 K (vs SCE).

and the redox potentials with peak separations are listed in Table 5. The cyclic voltammogram of [Mn^{IV}(Me₂Bcyclen)-

Table 5. Redox Potentials of [Mn^{IV}(Me₂Bcyclen)(OH)₂](PF₆)₂ Complexes under Argon (vs SCE)^a

redox couple	<i>E</i> _{1/2} (V)	peak separation (mV)
Mn ^V /Mn ^{IV}	+0.893	90
Mn ^{IV} /Mn ^{III}	+0.410	128
Mn ^{III} /Mn ^{II}	-0.793	285

^aConditions: solvent, acetonitrile; manganese(IV) complexes, 2 mM; tetrabutylammonium perchlorate, 0.1 M; 298 K.

(OH)₂](PF₆)₂ in dry acetonitrile reveals a Mn^{III}/Mn^{II} couple of -0.793 V (vs SCE) with a peak separation of 285 mV, a Mn^{IV}/Mn^{III} couple of 0.410 V (vs SCE) with a peak separation of 128 mV, and a Mn^V/Mn^{IV} couple of +0.893 V (vs SCE) with a peak separation of 90 mV. Apparently, this manganese(IV) complex is a gentle oxidant, similar to its analogue, Mn^{IV}(Me₂EBC)-(OH)₂(PF₆)₂. The EPR spectrum of [Mn^{IV}(Me₂Bcyclen)-(OH)₂](PF₆)₂ in dry acetonitrile at 130 K reveals two broad resonances at *g* values of 2.52 and 4.32, which further supports its monomeric manganese(IV) oxidation state (Figure 6), because these values are similar to those of its analogue, Mn^{IV}(Me₂EBC)(OH)₂(PF₆)₂, and other monomeric manganese(IV) complexes like [Mn(HB(3,5-Me₂pz)₃)₂](ClO₄)₄ (pz = pyrazolyl) reported in the literature.^{25,29}

Catalytic Reactivity of the Manganese(IV) Complex with Ca²⁺. Very interestingly, using the synthetic manganese(IV) complex in place of the corresponding manganese(II) complex as the catalyst generates more efficient sulfide oxidation. At 303 K, manganese(IV) alone as the catalyst displays a very fast catalytic rate, which makes it difficult to study with added Ca²⁺. Thus, a relatively low temperature, 273 K, was applied for this study to slow the oxidation rate. For comparison, the results are listed in Table 6. Compared with the Mn^{II}(Me₂Bcyclen)Cl₂ catalyst plus Ca²⁺, which needs 6 h at 303 K to achieve 91.4% conversion of thioanisole with 44.1% yield of sulfoxide and 37.1% yield of sulfone, the manganese-

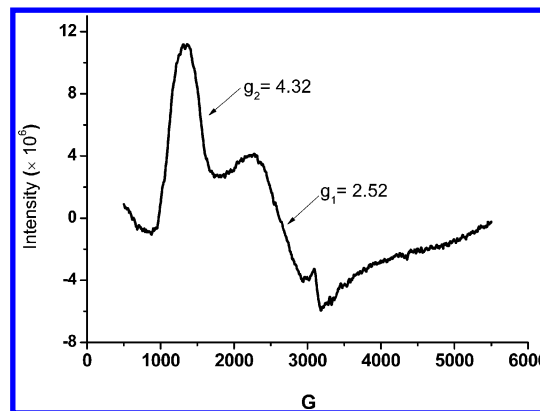


Figure 6. EPR spectra of the manganese(IV) complexes in dry acetonitrile at 130 K.

(IV) complex catalyst alone at 273 K (ice H₂O conditions) can give similar results in only 4 h, that is, 85.3% conversion, 36.3% yield of sulfoxide, and 45.0% yield of sulfone. Furthermore, in the presence of 1 equiv of Ca²⁺ at 273 K, the manganese(IV) complex gives complete conversion (99.0%) of substrate with 24.5% yield of sulfoxide and 65.7% yield of sulfone in 4 h. Notably, the yield of sulfone is much higher than that of sulfoxide, which is different from catalytic oxidation by the manganese(II) complex in the presence of Ca²⁺. As disclosed above, the manganese(IV) complex was quantitatively synthesized by oxidation of the corresponding manganese(II) complex with H₂O₂ in the presence of NH₄PF₆. Thus, a similar manganese(IV) species should exist under the sulfide oxidation conditions. One clear difference between the manganese(II) complex and the corresponding manganese(IV) complex as the catalyst, Mn^{II}(Me₂Bcyclen)Cl₂ vs Mn^{IV}(Me₂Bcyclen)(OH)₂(PF₆)₂, is that the former has chloride ligands, whereas the latter does not. In complementary experiments, adding 2 equiv of Ag(OTf) to Mn^{II}(Me₂Bcyclen)Cl₂ to generate the active Mn^{II}(Me₂Bcyclen)(OTf)₂ catalyst in situ provides 92.4% yield of sulfone with >99.9% conversion, and no sulfoxide was detected at 303 K. [Note: Although silver(0) formation is possible, which would generate a manganese(III) complex, neither black silver(0) precipitate nor characteristic brown manganese(III) catalyst color was observed.] In the case of the addition of 1 equiv of Ag(OTf) to generate in situ what could be represented stoichiometrically as the Mn^{II}(Me₂Bcyclen)Cl(OTf) catalyst (although we are not claiming this is the actual solution structure), it provides 12.6% yield of sulfoxide and 75.7% yield of sulfone with 99.6% conversion. In another test using CaCl₂ in place of Ca(OTf)₂, Mn^{IV}(Me₂Bcyclen)(OH)₂(PF₆)₂ as the catalyst provides only 25.6% yield of sulfoxide and 12.6% yield of sulfone with 41.2% conversion at 273 K, which is almost identical with that using Mn^{II}(Me₂Bcyclen)Cl₂ as the catalyst in the presence of Ca(OTf)₂, which provides 24.7% yield of sulfoxide and 10.7% yield of sulfone with 37.7% conversion at 273 K. Apparently, the presence of Cl⁻ decreases the catalytic activity of these manganese catalysts in sulfide oxidation, and the presence of Ca²⁺ may assist dissociation of the Cl⁻ anion, thus accelerating sulfide oxidation. However, the role of Ca²⁺ cannot be solely assigned to the abstraction of chloride from the manganese(II) complex because adding Ca²⁺ to the manganese(IV) complex, which has no chloride as a ligand, still improves its catalytic efficiency and shifts its redox potential (vide infra).

Table 6. Comparison of Catalytic Thioanisole Oxidation by $\text{Mn}^{\text{II}}(\text{Me}_2\text{Bcyclen})\text{Cl}_2$ and $\text{Mn}^{\text{IV}}(\text{Me}_2\text{Bcyclen})(\text{OH})_2(\text{PF}_6)_2$ Catalysts in the Presence of Ca^{2+} ^a

catalyst	additive	time (h)	temperature (K)	conversion (%)	yield of monoxide (%)	yield of dioxide (%)
Mn^{II}		6	303	65.9	32.6	25.9
Mn^{II}	$\text{Ca}(\text{OTf})_2$	6	303	91.4	44.1	37.1
Mn^{IV}		4	273	85.3	36.3	45.0
Mn^{IV}	$\text{Ca}(\text{OTf})_2$	4	273	99.0	24.5	65.7
Mn^{II}	$\text{Ca}(\text{OTf})_2$	4	273	37.7	24.7	10.7
Mn^{IV}	CaCl_2	4	273	41.2	25.6	12.6

^aConditions: solvent, acetonitrile 5 mL; thioanisole, 0.1 M; manganese(II) or manganese(IV) catalyst, 0.33 mM; $\text{Ca}(\text{OTf})_2$ or CaCl_2 , 0.33 mM; H_2O_2 , 0.2 mL.

Influence of Ca^{2+} and Cl^- on the Redox Potentials of Various Manganese Complexes. Although the role of Cl^- in oxygen evolution from PSII is still elusive, Sandusky and Yocum found that Cl^- is required for $\text{S}_2 \rightarrow \text{S}_3$ and $\text{S}_3 \rightarrow \text{S}_0$ transitions and proposed that Cl^- is possibly related to the electron-transfer event happening in the OEC.^{12a} Batista et al. also proposed that Cl^- is possibly related to proton transfer in the catalytic cycle.^{13a} Up to now, there has been no reported example to confirm the binding site of Cl^- in PSII or to demonstrate how Cl^- affects the redox potential of the Mn_4CaO_5 core in PSII. Generally, the thermodynamic driving force of an active species for electron transfer is directly related to its redox potential. Here, how Cl^- and Ca^{2+} together affect the redox potentials of a series of manganese ions in synthetic models including $\text{Mn}^{\text{II}}(\text{Me}_2\text{EBC})\text{Cl}_2$, $\text{Mn}^{\text{II}}(\text{Me}_2\text{Bcyclen})\text{Cl}_2$, $\text{Mn}^{\text{II}}(\text{TPA})\text{Cl}_2$, and $\text{Mn}^{\text{II}}(\text{BPMEN})\text{Cl}_2$ is investigated. Their cyclic voltammograms are shown in Figures 7 and 9, and related redox potentials are summarized in Tables 7 and 8.

Table 7. Influence of Ca^{2+} on the Redox Potential of Manganese(IV) Complexes (vs SCE)^a

		$E_{1/2}$ (V)	
		$\text{Mn}^{\text{V}}/\text{Mn}^{\text{IV}}$	$\text{Mn}^{\text{IV}}/\text{Mn}^{\text{III}}$
$\text{Mn}^{\text{IV}}(\text{Me}_2\text{EBC})(\text{OH})_2^{2+}$		+0.971	+0.461
$\text{Mn}^{\text{IV}}(\text{Me}_2\text{EBC})(\text{OH})_2^{2+}$	$\text{Ca}(\text{OTf})_2$	+0.959	+0.483
$\text{Mn}^{\text{IV}}(\text{Me}_2\text{Bcyclen})(\text{OH})_2^{2+}$		+0.893	+0.410
$\text{Mn}^{\text{IV}}(\text{Me}_2\text{Bcyclen})(\text{OH})_2^{2+}$	$\text{Ca}(\text{OTf})_2$	+0.855	+0.455

^aConditions: solvent, dry acetonitrile; manganese(IV) complexes, 2 mM; $\text{Ca}(\text{OTf})_2$, 2 mM; tetrabutylammonium perchlorate, 0.1 M; under argon at 298 K.

Table 8. Influence of Ca^{2+} and Cl^- on the Redox Potentials of Manganese(II) Complexes^a

		$E_{1/2}$ (V)	
		$\text{Mn}^{\text{V}}/\text{Mn}^{\text{IV}}$	$\text{Mn}^{\text{IV}}/\text{Mn}^{\text{III}}$
$\text{Mn}^{\text{II}}(\text{TPA})\text{Cl}_2$		+1.550	+0.795
$\text{Mn}^{\text{II}}(\text{TPA})\text{Cl}_2$	$\text{Ca}(\text{OTf})_2$	+1.482	+0.775
$\text{Mn}^{\text{II}}(\text{BPMEN})\text{Cl}_2$		+1.504	+0.762
$\text{Mn}^{\text{II}}(\text{BPMEN})\text{Cl}_2$	$\text{Ca}(\text{OTf})_2$	+1.480	+0.737
$\text{Mn}^{\text{II}}(\text{Me}_2\text{EBC})\text{Cl}_2$		+1.321	+0.599
$\text{Mn}^{\text{II}}(\text{Me}_2\text{EBC})\text{Cl}_2$	$\text{Ca}(\text{OTf})_2$	+1.274	+0.563
$\text{Mn}^{\text{II}}(\text{Me}_2\text{Bcyclen})\text{Cl}_2$		+1.218	+0.465
$\text{Mn}^{\text{II}}(\text{Me}_2\text{Bcyclen})\text{Cl}_2$	$\text{Ca}(\text{OTf})_2$	+1.174	+0.444

^aConditions: solvent, dry acetonitrile; manganese(II) complexes, 2 mM; $\text{Ca}(\text{OTf})_2$, 2 mM; tetrabutylammonium perchlorate, 0.1 M; under argon at 298 K.

Both manganese(IV) complexes of Me_2EBC and $\text{Me}_2\text{Bcyclen}$ have two hydroxide ligands, and there is no chloride present under electrochemical conditions. One may see in Figure 7 that

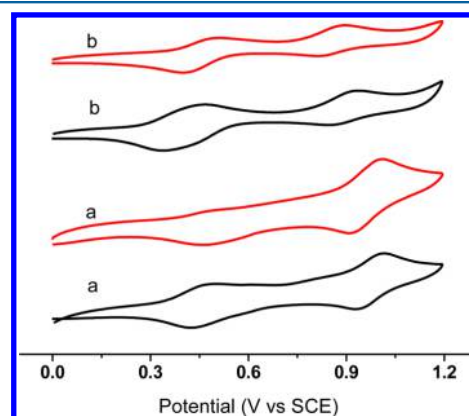


Figure 7. Influence of Ca^{2+} on the electrochemical behaviors of $\text{Mn}^{\text{IV}}(\text{Me}_2\text{Bcyclen})(\text{OH})_2(\text{PF}_6)_2$ and $\text{Mn}^{\text{IV}}(\text{Me}_2\text{EBC})(\text{OH})_2(\text{PF}_6)_2$ in dry acetonitrile under argon at 298 K. Conditions: manganese(IV) complexes, 2 mM; $\text{Ca}(\text{OTf})_2$, 2 mM; tetrabutylammonium perchlorate, 0.1 M; (a) $\text{Mn}^{\text{IV}}(\text{Me}_2\text{EBC})(\text{OH})_2(\text{PF}_6)_2$; (b) $\text{Mn}^{\text{IV}}(\text{Me}_2\text{Bcyclen})(\text{OH})_2(\text{PF}_6)_2$. Black curves represent manganese(IV) complexes alone, and red ones represent manganese(IV) complexes with $\text{Ca}(\text{OTf})_2$.

adding 1 equiv of Ca^{2+} to the manganese(IV) complexes has clearly changed their redox potentials. However, the influence of Ca^{2+} on the $\text{Mn}^{\text{V}}/\text{Mn}^{\text{IV}}$ and $\text{Mn}^{\text{IV}}/\text{Mn}^{\text{III}}$ couples is inverted. For the $\text{Mn}^{\text{IV}}(\text{Me}_2\text{Bcyclen})(\text{OH})_2(\text{PF}_6)_2$ complex, the original potentials of the $\text{Mn}^{\text{IV}}/\text{Mn}^{\text{III}}$ and $\text{Mn}^{\text{V}}/\text{Mn}^{\text{IV}}$ couples are +0.410 and +0.893 V (vs SCE), respectively. In the presence of Ca^{2+} , the potential of the $\text{Mn}^{\text{IV}}/\text{Mn}^{\text{III}}$ couple positively shifts from 0.045 to +0.455 V (vs SCE), whereas for the $\text{Mn}^{\text{V}}/\text{Mn}^{\text{IV}}$ couple, it negatively shifts from 0.038 to +0.855 V (vs SCE). However, varying the concentration of Ca^{2+} does not further shift the potentials of the manganese(IV) complex, implying that there is only a single bimetallic $\text{Mn}^{\text{IV}}-\text{Ca}^{2+}$ adduct generated, and no multimetallic adduct formation from adding more Ca^{2+} (see Figure S2 in the SI for details). For comparison, the influence of Ca^{2+} on the redox potentials of its analogue, $\text{Mn}^{\text{IV}}(\text{Me}_2\text{EBC})(\text{OH})_2(\text{PF}_6)_2$, has also been investigated, and similar shifts have been confirmed in the presence of Ca^{2+} . That is, adding Ca^{2+} negatively shifts the $\text{Mn}^{\text{V}}/\text{Mn}^{\text{IV}}$ couple from +0.971 to +0.959 V (vs SCE) but positively shifts the $\text{Mn}^{\text{IV}}/\text{Mn}^{\text{III}}$ couple from +0.461 to +0.483 V (vs SCE). Clearly, there are distinctly different influences of Ca^{2+} on the $\text{Mn}^{\text{V}}/\text{Mn}^{\text{IV}}$ and $\text{Mn}^{\text{IV}}/\text{Mn}^{\text{III}}$ couples. In complementary experiments, it was found that other mild Lewis acid alkaline-earth metals, Mg^{2+} ,

Sr^{2+} , and Ba^{2+} , have similar influences on the redox potentials of the manganese(IV) complex as Ca^{2+} does (see Figure S3 in the SI for details). While not included in this study of mild Lewis acids focusing on Ca^{2+} , the literature teaches us that much stronger Lewis acids like Sc^{3+} and Al^{3+} shift the potentials of manganese(IV) complexes more obviously, but they also make the manganese(IV) species less stable.^{19h}

Agapie and co-workers recently reported a series of heterometallic manganese oxido cubane clusters in which redox-inactive metal ions significantly affect the redox potential of the manganese ions in clusters.^{6a,e} Particularly, the synthetic $\text{Mn}^{\text{IV}}_3\text{CaO}_4$ complex demonstrated a much more negative potential compared with the all-manganese $\text{Mn}^{\text{IV}}_3\text{Mn}^{\text{III}}\text{O}_4$ cluster, suggesting that the presence of Ca^{2+} in the cluster may facilitate access of the high oxidation state of manganese centers at a relatively low potential level during the S-state transition. Here, in this monomeric manganese(IV) model, the presence of Ca^{2+} also shifts the potential of the $\text{Mn}^{\text{V}}/\text{Mn}^{\text{IV}}$ couple negatively. However, it also positively shifts the potential of the $\text{Mn}^{\text{IV}}/\text{Mn}^{\text{III}}$ couple under electrochemical conditions.

The highest oxidation state of the manganese ions in the S_4 state is still controversial in the OEC. In theoretical studies, it generally proposed that all of the manganese ions in the S_4 state are in the 4+ oxidation state.^{9,10} Brudvig and co-workers have suggested that the monomeric manganese appendage is in a $\text{Mn}^{\text{V}}=\text{O}$ or $\text{Mn}^{\text{IV}}\text{O}^\bullet$ form, which is proposed to be involved in O–O bond formation in the S_4 state.^{7a,b} Here, the different influences of Ca^{2+} on the redox potentials of the $\text{Mn}^{\text{V}}/\text{Mn}^{\text{III}}$ and $\text{Mn}^{\text{V}}/\text{Mn}^{\text{IV}}$ couples may provide new clues for understanding the related oxidation development in the OEC.

The positively shifted potential of the $\text{Mn}^{\text{IV}}/\text{Mn}^{\text{III}}$ couple upon the addition of Ca^{2+} may be expected to improve its oxidation capability. For example, although manganese(IV) alone, or in the presence of Ca^{2+} , cannot quantitatively oxidize sulfide to sulfoxide, adding Ca^{2+} can promote its oxygenation efficiency on triphenylphosphine. In acetonitrile at 298 K, oxygenation of triphenylphosphine by the $\text{Mn}^{\text{IV}}(\text{Me}_2\text{Bcyclen})(\text{OH})_2(\text{PF}_6)_2$ complex yields 54.5% of the oxide product in 4 h based on the manganese(IV) complex added. Adding 1 equiv of Ca^{2+} improves the yield up to 73.8%. The oxygenation kinetics does not fit a simple first-order rate for the disappearance of the manganese(IV) species, implying the formation of a precomplex between the manganese(IV) complex and triphenylphosphine prior to oxygenation. However, the kinetic data still demonstrate that adding Ca^{2+} can accelerate the oxygenation rate (see Table S5 and Figure S4 in the SI for details). Although the Hammett plot of substituted triphenylphosphine was not available because of the complicated oxygenation kinetics, according to the oxygenation mechanism of its analogue, $\text{Mn}^{\text{IV}}(\text{Me}_2\text{EBC})(\text{OH})_2(\text{PF}_6)_2$,^{19a,d} it can be rationally proposed that, here, the oxygenation of triphenylphosphine also proceeds by electron transfer, and adding Ca^{2+} may substantially accelerate its electron transfer because of its increased potential. Notably, the control experiment shows that manganese(IV) alone is not indefinitely stable under the reaction conditions, which is consistent with it being a gentle oxidant having a potential of +0.41 V (vs SCE).

The UV–vis spectrum provides evidence for the interaction of Ca^{2+} with $\text{Mn}^{\text{IV}}(\text{Me}_2\text{Bcyclen})(\text{OH})_2^{2+}$. As shown in Figure 8, $\text{Mn}^{\text{IV}}(\text{Me}_2\text{Bcyclen})(\text{OH})_2^{2+}$ alone demonstrates a characteristic absorbance at 589 nm with a ϵ value of $682 \text{ M}^{-1} \text{ cm}^{-1}$. Adding 1 equiv of Ca^{2+} generates a blue shift of this absorbance of the characteristic manganese(IV) species at 577 nm having a ϵ

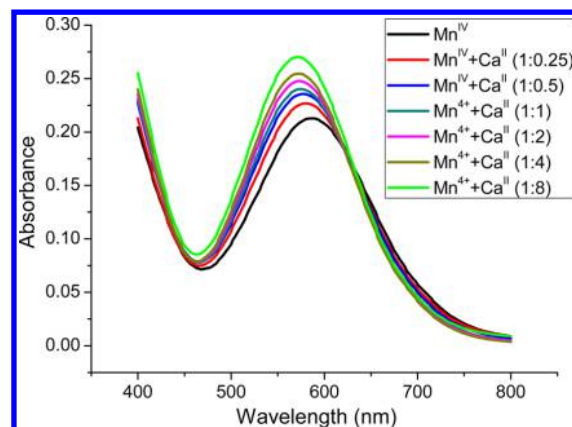


Figure 8. UV–vis spectra of the manganese(IV) complexes (0.33 mM) in the presence of different concentrations of $\text{Ca}(\text{OTf})_2$ in acetonitrile at 298 K.

value of $777 \text{ M}^{-1} \text{ cm}^{-1}$. Interestingly, increasing the Ca^{2+} concentration beyond 1:1 changes only the intensity of the new species and does not shift it further. A reasonable explanation is that there exists an equilibrium between the free manganese(IV) complex and a bimetallic $\text{Mn}^{\text{IV}}\text{--Ca}^{2+}$ adduct. Adding excess Lewis acid shifts this equilibrium toward the bimetallic adduct, thus increasing its absorbance, but generates no additional multimetallic adducts. This explanation (formation of a bimetallic adduct with no further multimetallic adduct formed by adding more than 1:1 Ca^{2+}) is also consistent with the results of the electrochemical studies (vide supra). In complementary experiments, adding Mg^{2+} , Sr^{2+} , and Ba^{2+} also blue-shifts the absorbance of the manganese(IV) species (see Figure S5 in the SI in details). A similar blue shift was previously observed upon the addition of Al^{3+} to the solution of the $\text{Mn}^{\text{IV}}(\text{Me}_2\text{EBC})(\text{OH})_2(\text{PF}_6)_2$ complex, which caused its characteristic absorbance of manganese(IV) species to shift from 554 to 537 nm.^{19h} Thereof, the bimetallic $\text{Mn}^{\text{IV}}\text{--Ca}^{2+}$ adduct can be putatively proposed as forming a $\text{Mn}^{\text{IV}}\text{--O--Ca}^{2+}$ bridge through Ca^{2+} -assisted deprotonation of the $\text{Mn}^{\text{IV}}\text{--OH}$ moiety, similar to that formed by Al^{3+} with the related $\text{Mn}^{\text{IV}}(\text{Me}_2\text{EBC})(\text{OH})_2(\text{PF}_6)_2$ complex.

To address the influence of both Ca^{2+} and Cl^- on the redox potentials of the manganese ion, the electrochemical behaviors of a series of manganese(II) complexes having chloride ligand including $\text{Mn}^{\text{II}}(\text{Me}_2\text{EBC})\text{Cl}_2$, $\text{Mn}^{\text{II}}(\text{Me}_2\text{Bcyclen})\text{Cl}_2$, $\text{Mn}^{\text{II}}(\text{TPA})\text{Cl}_2$, and $\text{Mn}^{\text{II}}(\text{BPMEN})\text{Cl}_2$ were investigated, and the cyclic voltammograms are shown in Figure 9 and their redox potentials are summarized in Table 8. Unlike the above-discussed manganese(IV) complexes having two hydroxide ligands, the presence of Ca^{2+} negatively shifts the redox potentials of all of the $\text{Mn}^{\text{V}}/\text{Mn}^{\text{IV}}$ and $\text{Mn}^{\text{IV}}/\text{Mn}^{\text{III}}$ couples for the four tested manganese(II) complexes having two chloride ligands. For example, the original redox potentials of the $\text{Mn}^{\text{V}}/\text{Mn}^{\text{IV}}$ and $\text{Mn}^{\text{IV}}/\text{Mn}^{\text{III}}$ couples in the $\text{Mn}(\text{Me}_2\text{Bcyclen})\text{Cl}_2$ complexes are +1.218 and +0.465 V (vs SCE), respectively. In the presence of 1 equiv of Ca^{2+} , its potential for the $\text{Mn}^{\text{V}}/\text{Mn}^{\text{IV}}$ couple negatively shifts by 0.044 to +1.174 V (vs SCE), and the potential also negatively shifts by 0.021 to +0.444 V (vs SCE) for the $\text{Mn}^{\text{IV}}/\text{Mn}^{\text{III}}$ couple. In addition, increasing the Ca^{2+} concentration above 1:1 slightly shifts the potentials of the manganese(II) complex further, possibly related to an enhanced ability of Ca^{2+} in the removal of Cl^- from the manganese(II) complex (see Figure S6 in the SI for details).

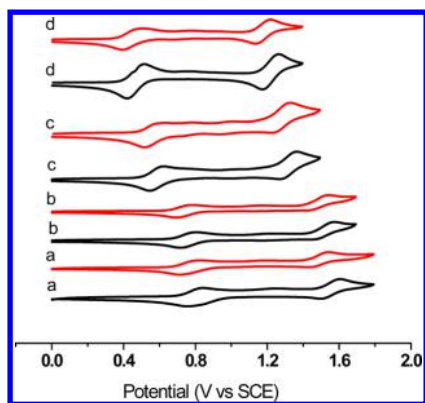


Figure 9. Influence of Ca^{2+} on the electrochemical behaviors of manganese(II) complexes having chloride ligands. Conditions: solvent, dry acetonitrile; manganese(II) complexes, 2 mM; $\text{Ca}(\text{OTf})_2$, 2 mM; tetrabutylammonium perchlorate, 0.1 M; under argon at 298 K; (a) $\text{Mn}^{\text{II}}(\text{TPA})\text{Cl}_2$; (b) $\text{Mn}^{\text{II}}(\text{BPMEN})\text{Cl}_2$; (c) $\text{Mn}^{\text{II}}(\text{Me}_2\text{cyclam})\text{Cl}_2$; (d) $\text{Mn}^{\text{II}}(\text{Me}_2\text{Bcyclen})\text{Cl}_2$. Black curves represent manganese(II) complexes alone, and red ones represent the manganese(II) complexes with $\text{Ca}(\text{OTf})_2$.

Although the shifted values are not large, the identical shifting tendency of four examined manganese(II) complexes makes the trend convincing. In complementary experiments, it was found that Mg^{2+} , Sr^{2+} , and Ba^{2+} have similar influences on the redox potentials of $\text{Mn}(\text{Me}_2\text{Bcyclen})\text{Cl}_2$. That is, all of them negatively shift the potential of the $\text{Mn}^{\text{V}}/\text{Mn}^{\text{IV}}$ and $\text{Mn}^{\text{IV}}/\text{Mn}^{\text{III}}$ couples in the manganese(II) complex (see Figure S7 in the SI for details).

Currently, the accurate binding site of Cl^- in the OEC during the catalytic cycle still remains elusive. The proposed potential role of Cl^- in the OEC is related to electron transfer, proton transfer, regulation of the potential of the OEC, and activation of substrate H_2O .^{11–13} Here, the presence of Cl^- also affects the potentials of manganese complexes and even reverses the influence of Ca^{2+} on the $\text{Mn}^{\text{IV}}/\text{Mn}^{\text{III}}$ couple. For example, adding Ca^{2+} positively shifts the redox potential of the $\text{Mn}^{\text{IV}}/\text{Mn}^{\text{III}}$ couple in the $\text{Mn}^{\text{IV}}(\text{Me}_2\text{Bcyclen})(\text{OH})_2(\text{PF}_6)_2$ complex from +0.410 to +0.455 V (vs SCE), which is in the opposite direction to the shift of the $\text{Mn}^{\text{V}}/\text{Mn}^{\text{IV}}$ couple. In the corresponding $\text{Mn}^{\text{II}}(\text{Me}_2\text{Bcyclen})\text{Cl}_2$ complex, adding Ca^{2+} negatively shifts the $\text{Mn}^{\text{IV}}/\text{Mn}^{\text{III}}$ couple from +0.465 to +0.444 V (vs SCE), demonstrating a tendency similar to that of the $\text{Mn}^{\text{V}}/\text{Mn}^{\text{IV}}$ couple with Ca^{2+} alone. Because chloride salts like CaCl_2 , LiCl , and NaCl are not soluble in acetonitrile, how Cl^- affects the redox chemistry of the manganese(IV) complex in acetonitrile is not accessible. Alternatively, LiCl is soluble in acetone, and the influence of Cl^- on the potentials of the manganese(IV) complex was investigated in acetone. As shown in Figure S8 in the SI, adding Cl^- to the $\text{Mn}^{\text{IV}}(\text{Me}_2\text{Bcyclen})(\text{OH})_2(\text{PF}_6)_2$ complex positively shifts both of the $\text{Mn}^{\text{V}}/\text{Mn}^{\text{IV}}$ and $\text{Mn}^{\text{IV}}/\text{Mn}^{\text{III}}$ couples from +0.930 and +0.503 V (vs SCE) to +1.014 and +0.528 V (vs SCE), respectively, while subsequently adding $\text{Ca}(\text{OTf})_2$ to the solution containing the manganese(IV) complex and LiCl reverses the trend in the redox potential shift, that is, shifting both potentials negatively from +1.014 and +0.528 V (vs SCE) to +0.992 and +0.487 V (vs SCE), respectively. Taken together, the presence of Ca^{2+} can affect the binding of the Cl^- anion to both manganese(II) and manganese(IV) complexes, thus synergistically affecting the redox potentials of manganese and

modulating its oxidative reactivity. Even in the absence of Cl^- , Ca^{2+} can also affect the reactivity of manganese through its linkage to the high-oxidation-state manganese ion. Although the influence of Ca^{2+} and Cl^- on the redox potentials and reactivity of the manganese complexes in this work may not directly reflect their roles in the OEC, it may provide new clues to understanding their roles in dioxygen evolution in the OEC of PSII.

CONCLUSIONS

Through catalytic sulfide oxidations by the $\text{Mn}^{\text{II}}(\text{Me}_2\text{Bcyclen})\text{Cl}_2$ complex in the presence/absence of Ca^{2+} , it has been found that adding Ca^{2+} substantially improves the oxygenation efficiency of the manganese(II) catalyst and accelerates the conversion of sulfoxide to sulfone. Similar acceleration effects have also been observed for Mg^{2+} , Sr^{2+} , and Ba^{2+} . Using an isolated and well-characterized $\text{Mn}^{\text{IV}}(\text{Me}_2\text{Bcyclen})(\text{OH})_2(\text{PF}_6)_2$ complex as the catalyst, it was found that this manganese(IV) catalyst demonstrates more efficient catalytic activity than the corresponding manganese(II) complex. Conclusively, adding Ca^{2+} further improves its efficiency, yet adding Cl^- to the manganese(IV) complex, which has no chloride ligand, will decrease its catalytic activity. Detailed electrochemical studies revealed that adding Ca^{2+} to monomeric manganese(IV) complexes, which have no chloride ligand, shifts the $\text{Mn}^{\text{IV}}/\text{Mn}^{\text{III}}$ couple positively, whereas it shifts the $\text{Mn}^{\text{V}}/\text{Mn}^{\text{IV}}$ couple negatively. Notably, adding Cl^- to the manganese(IV) complex positively shifts its $\text{Mn}^{\text{V}}/\text{Mn}^{\text{IV}}$ and $\text{Mn}^{\text{IV}}/\text{Mn}^{\text{III}}$ couples, whereas further adding Ca^{2+} will reverse that trend, negatively shifting both couples. In the tested manganese(II) complexes, which contain chloride, adding Ca^{2+} shifts both the $\text{Mn}^{\text{V}}/\text{Mn}^{\text{IV}}$ and $\text{Mn}^{\text{IV}}/\text{Mn}^{\text{III}}$ couples to the negative direction, thus demonstrating different influences of Ca^{2+} and Cl^- on the redox behaviors of the manganese ions.

ASSOCIATED CONTENT

Supporting Information

X-ray crystallographic data in CIF format, catalytic sulfide oxidation under different conditions, GC–MS graphs of the C–S cleavage products of benzyl phenyl sulfide in catalytic oxidations, detailed electrochemical results, and detailed crystal data for $\text{Mn}^{\text{IV}}(\text{Me}_2\text{Bcyclen})(\text{OH})_2(\text{PF}_6)_2$. This material is available free of charge via the Internet at <http://pubs.acs.org>.

AUTHOR INFORMATION

Corresponding Authors

*E-mail: tim.hubin@swosu.edu.

*E-mail: gyin@hust.edu.cn.

Notes

The authors declare no competing financial interest.

ACKNOWLEDGMENTS

GC–MS analysis was performed in the Analytical and Testing Center of Huazhong University of Science and Technology. This work was supported by the National Natural Science Foundation of China (Grants 21273086 and 21303063). T.J.H. acknowledges the donors of the American Chemical Society Petroleum Research Fund for partial support of this research. T.J.H. also acknowledges the Henry Dreyfus Teacher–Scholar Awards Program for support of this work.

REFERENCES

- (1) (a) Sproviero, E. M.; Gascón, J. A.; McEvoy, J. P.; Brudvig, G. W.; Batista, V. S. *Coord. Chem. Rev.* **2008**, 252, 395. (b) Vrettos, J. S.; Limburg, J.; Brudvig, G. W. *Biochim. Biophys. Acta* **2001**, 1503, 229. (c) Najafpour, M. M.; Govindjee. *Dalton Trans.* **2011**, 40, 9076. (d) McEvoy, J. P.; Brudvig, G. W. *Chem. Rev.* **2006**, 106, 4455.
- (2) (a) Sheats, J. E.; Czernuszewicz, R. S.; Dismukes, G. C.; Rheingold, A. L.; Petrouleas, V.; Stubbe, J.; Armstrong, W. H.; Beer, R. H.; Lippard, S. J. *J. Am. Chem. Soc.* **1987**, 109, 1435. (b) Chen, H.; Faller, J. W.; Crabtree, R. H.; Brudvig, G. W. *J. Am. Chem. Soc.* **2004**, 126, 7345. (c) Pecoraro, V. L.; Hsieh, W. *Inorg. Chem.* **2008**, 47, 1765. (d) Zaleski, C. M.; Weng, T.; Dendrinou-Samara, C.; Alexiou, M.; Kanakarakis, P.; Hsieh, W.; Kampf, J.; Penner-Hahn, J. E.; Pecoraro, V. L.; Kessissoglou, D. P. *Inorg. Chem.* **2008**, 47, 6127.
- (3) (a) Mukhopadhyay, S.; Mandal, S. K.; Bhaduri, S.; Armstrong, W. H. *Chem. Rev.* **2004**, 104, 3981. (b) Najafpour, M. M. *J. Photochem. Photobiol., B* **2011**, 104, 111. (c) Carrell, T. G.; Tyryshkin, A. M.; Dismukes, G. C. *J. Biol. Inorg. Chem.* **2002**, 7, 2. (d) McAlpin, J. G.; Stich, T. A.; Casey, W. H.; Britt, R. D. *Coord. Chem. Rev.* **2012**, 256, 2445. (e) Mullins, C. S.; Pecoraro, V. L. *Coord. Chem. Rev.* **2008**, 252, 416. (f) Hurst, J. K. *Coord. Chem. Rev.* **2005**, 249, 313. (g) Dismukes, G. C.; Brimblecombe, R.; Felton, G. A. N.; Pryadun, R. S.; Sheats, J. E.; Spiccia, L.; Swiegers, G. F. *Acc. Chem. Res.* **2009**, 42, 1935. (h) Sala, X.; Maji, S.; Boffill, R.; Garcia-Anton, J.; Escriche, L.; Llobet, A. *Acc. Chem. Res.* **2014**, 47, 504. (i) Sartorel, A.; Bonchio, M.; Campagna, S.; Scandola, F. *Chem. Soc. Rev.* **2013**, 42, 2262. (j) Yagi, M.; Kaneko, M. *Chem. Rev.* **2001**, 101, 21.
- (4) (a) Boussac, A.; Zimmermann, J. L.; Rutherford, A. W. *Biochemistry* **1989**, 28, 8984. (b) Sivaraja, M.; Tso, J.; Dismukes, G. C. *Biochemistry* **1989**, 28, 9459. (c) Ono, T. A.; Inoue, Y. *Arch. Biochem. Biophys.* **1989**, 275, 440. (d) Hallahan, B. J.; Nugent, J. H. A.; Warden, J. T.; Evans, M. C. W. *Biochemistry* **1992**, 31, 4562. (e) Gilchrist, M. L.; Ball, J. A.; Randall, D. W.; Britt, R. D. *Proc. Natl. Acad. Sci. U.S.A.* **1995**, 92, 9545. (f) Lydakis-Simantiris, N.; Dorlet, P.; Ghanotakis, D. F.; Babcock, G. T. *Biochemistry* **1998**, 37, 6427. (g) Yocum, C. F. *Coord. Chem. Rev.* **2008**, 252, 296. (h) Dasgupta, J.; van Willigen, R. T.; Dismukes, G. C. *Phys. Chem. Chem. Phys.* **2004**, 6, 4793. (i) Yachandra, V. K.; Yano, J. *J. Photochem. Photobiol., B* **2011**, 104, 51.
- (5) Miqyass, M.; Marosvölgyi, M. A.; Nagel, Z.; Yocum, C. F.; van Gorkom, H. J. *Biochemistry* **2008**, 47, 7915.
- (6) (a) Kanady, J. S.; Tsui, E. Y.; Day, M. W.; Agapie, T. *Science* **2011**, 333, 733. (b) Mukherjee, S.; Stull, J. A.; Yano, J.; Stamatatos, T. C.; Pringouri, K.; Stich, T. A.; Abboud, K. A.; Britt, R. D.; Yachandra, V. K.; Christou, G. *Proc. Natl. Acad. Sci. U.S.A.* **2012**, 109, 2257. (c) Kanady, J. S.; Mendoza-Cortes, J. L.; Tsui, E. Y.; Nielsen, R. J.; Goddard, W. A., III; Agapie, T. *J. Am. Chem. Soc.* **2013**, 135, 1073. (d) Tsui, E. Y.; Tran, R.; Yano, J.; Agapie, T. *Nat. Chem.* **2013**, 5, 293. (e) Tsui, E. Y.; Agapie, T. *Proc. Natl. Acad. Sci. U.S.A.* **2013**, 110, 10084.
- (7) (a) Pecoraro, V. L.; Baldwin, M. J.; Caudle, M. T.; Hsieh, W.-Y.; Law, N. A. *Pure Appl. Chem.* **1998**, 70, 925. (b) Lee, C. I.; Lakshmi, K. V.; Brudvig, G. W. *Biochemistry* **2007**, 46, 3211.
- (8) Ferreira, K. N.; Iverson, T. M.; Maghlaoui, K.; Barber, J.; Iwata, S. *Science* **2004**, 303, 1831.
- (9) Sproviero, E. M.; Gascón, J. A.; McEvoy, J. P.; Brudvig, G. W.; Batista, V. S. *J. Am. Chem. Soc.* **2008**, 130, 3428.
- (10) (a) Siegbahn, P. E. M.; Crabtree, R. H. *J. Am. Chem. Soc.* **1999**, 121, 117. (b) Siegbahn, P. E. M. *J. Photochem. Photobiol., B* **2011**, 104, 94.
- (11) (a) Murray, J. W.; Maghlaoui, K.; Kargul, J.; Ishida, N.; Lai, T. L.; Rutherford, A. W.; Sugiura, M.; Boussac, A.; Barber, J. *Energy Environ. Sci.* **2008**, 1, 161. (b) Kawakami, K.; Umena, Y.; Kamiya, N.; Shen, J. R. *Proc. Natl. Acad. Sci. U.S.A.* **2009**, 106, 8567. (c) Guskov, A.; Kern, J.; Gabdulkhakov, A.; Broser, M.; Zouni, A.; Saenger, W. *Nat. Struct. Mol. Biol.* **2009**, 16, 334. (d) Haumann, M.; Barra, M.; Loja, P.; Löscher, S.; Krivanek, R.; Grundmeier, A.; Andreasson, L.; Dau, H. *Biochemistry* **2006**, 45, 13101.
- (12) (a) Sandusky, P. O.; Yocum, C. F. *Biochim. Biophys. Acta* **1984**, 766, 603. (b) Wincencjusz, H.; van Gorkom, H. J.; Yocum, C. F. *Biochemistry* **1997**, 36, 3663. (c) Boussac, A.; Rutherford, A. W. *J. Biol. Chem.* **1994**, 269, 12462.
- (13) (a) Rivalta, I.; Amin, M.; Lubner, S.; Vassiliev, S.; Pokhrel, R.; Umena, Y.; Kawakami, K.; Shen, J.; Kamiya, N.; Bruce, D.; Brudvig, G. W.; Gunner, M. R.; Batista, V. S. *Biochemistry* **2011**, 50, 6312. (b) Pokhrel, R.; Service, R. J.; Debus, R. J.; Brudvig, G. W. *Biochemistry* **2013**, 52, 4758.
- (14) (a) Park, Y. J.; Cook, S. A.; Sickerman, N. S.; Sano, Y.; Ziller, J. W.; Borovik, A. S. *Chem. Sci.* **2013**, 4, 717. (b) Park, Y. J.; Ziller, J. W.; Borovik, A. S. *J. Am. Chem. Soc.* **2011**, 133, 9258.
- (15) (a) Grasselli, R. K. *Top. Catal.* **2002**, 21, 79. (b) Gluhoi, A. C.; Lin, S. D.; Nieuwenhuys, B. E. *Catal. Today* **2004**, 90, 175. (c) Wachs, I. E.; Deo, G.; Jehng, J. M.; Kim, D. S.; Hu, H. *ACS Symp. Ser.* **1996**, 638, 292.
- (16) (a) Du, H.; Lo, P.; Hu, Z.; Liang, H.; Lau, K.; Wang, Y.; Lam, W. W. Y.; Lau, T. *Chem. Commun.* **2011**, 47, 7143. (b) Yiu, S.; Man, W.; Lau, T. *J. Am. Chem. Soc.* **2008**, 130, 10821. (c) Lam, W. W. Y.; Yiu, S.; Lee, J. M. N.; Yau, S. K. Y.; Kwong, H.; Lau, T.; Liu, D.; Lin, Z. *J. Am. Chem. Soc.* **2006**, 128, 2851. (d) Yiu, S.; Wu, Z.; Mak, C.; Lau, T. *J. Am. Chem. Soc.* **2004**, 126, 14921. (e) Ho, C.; Lau, T. *New J. Chem.* **2000**, 24, 587. (f) Lau, T.; Wu, Z.; Bai, Z.; Mak, C. *J. Chem. Soc., Dalton Trans.* **1995**, 4, 695. (g) Lau, T.; Mak, C. *J. Chem. Soc., Chem. Commun.* **1993**, 9, 766.
- (17) (a) Morimoto, Y.; Kotani, H.; Park, J.; Lee, Y.; Nam, W.; Fukuzumi, S. *J. Am. Chem. Soc.* **2011**, 133, 403. (b) Fukuzumi, S.; Morimoto, Y.; Kotani, H.; Naumov, P.; Lee, Y.; Nam, W. *Nat. Chem.* **2010**, 2, 756. (c) Fukuzumi, S.; Ohkubo, K.; Morimoto, Y. *Phys. Chem. Chem. Phys.* **2012**, 14, 8472. (d) Fukuzumi, S.; Ohkubo, K. *Coord. Chem. Rev.* **2010**, 254, 372. (e) Nam, W.; Lee, Y.; Fukuzumi, S. *Acc. Chem. Res.* **2014**, 47, 1146. (f) Fukuzumi, S. *Coord. Chem. Rev.* **2013**, 257, 1564. (g) Fukuzumi, S. *Chem. Lett.* **2008**, 37, 808. (h) Park, J.; Morimoto, Y.; Lee, Y.; Nam, W.; Fukuzumi, S. *J. Am. Chem. Soc.* **2011**, 133, 5236. (i) Yoon, H.; Lee, Y.; Wu, X.; Cho, K.; Sarangi, R.; Nam, W.; Fukuzumi, S. *J. Am. Chem. Soc.* **2013**, 135, 9186. (j) Park, J.; Morimoto, Y.; Lee, Y.; Nam, W.; Fukuzumi, S. *Inorg. Chem.* **2014**, 53, 3618.
- (18) (a) Leeladee, P.; Baglia, R. A.; Prokop, K. A.; Latifi, R.; de Visser, S. P.; Goldberg, D. P. *J. Am. Chem. Soc.* **2012**, 134, 10397. (b) Baglia, R. A.; Dürr, M.; Ivanović-Burmazović, I.; Goldberg, D. P. *Inorg. Chem.* **2014**, 53, 5893.
- (19) (a) Yin, G. *Acc. Chem. Res.* **2013**, 46, 483. (b) Wang, Y.; Sheng, J.; Shi, S.; Zhu, D.; Yin, G. *J. Phys. Chem. C* **2012**, 116, 13231. (c) Shi, S.; Wang, Y.; Xu, A.; Wang, H.; Zhu, D.; Roy, S. B.; Jackson, T. A.; Busch, D. H.; Yin, G. *Angew. Chem., Int. Ed.* **2011**, 50, 7321. (d) Xu, A.; Xiong, H.; Yin, G. *Chem.—Eur. J.* **2009**, 15, 11478. (e) Wang, Y.; Shi, S.; Wang, H.; Zhu, D.; Yin, G. *Chem. Commun.* **2012**, 48, 7832. (f) Yin, G.; Danby, A. M.; Kitko, D.; Carter, J. D.; Scheper, W. M.; Busch, D. H. *Inorg. Chem.* **2007**, 46, 2173. (g) Yin, G.; Danby, A. M.; Kitko, D.; Carter, J. D.; Scheper, W. M.; Busch, D. H. *J. Am. Chem. Soc.* **2008**, 130, 16245. (h) Dong, L.; Wang, Y.; Lv, Y.; Chen, Z.; Mei, F.; Xiong, H.; Yin, G. *Inorg. Chem.* **2013**, 52, 5418.
- (20) Hubin, T. J.; McCormick, J. M.; Collinson, S. R.; Buchalova, M.; Perkins, C. M.; Alcock, N. W.; Kahol, P. K.; Raghunathan, A.; Busch, D. H. *J. Am. Chem. Soc.* **2000**, 122, 2512.
- (21) Hitomi, Y.; Ando, A.; Matsui, H.; Ito, T.; Tanaka, T.; Ogo, S.; Funabiki, T. *Inorg. Chem.* **2005**, 44, 3473.
- (22) Hureau, C.; Blondin, G.; Charlot, M.; Philouze, C.; Nierlich, M.; Césario, M.; Anxolabéhère-Mallart, E. *Inorg. Chem.* **2005**, 44, 3669.
- (23) (a) Boussac, A.; Rutherford, A. W. *Biochemistry* **1988**, 27, 3476. (b) Ghanotakis, D. F.; Babcock, G. T.; Yocum, C. F. *FEBS Lett.* **1984**, 167, 127. (c) Boussac, A.; Sétif, P.; Rutherford, A. W. *Biochemistry* **1992**, 31, 1224. (d) Boussac, A.; Rappaport, F.; Carrier, P.; Verbavatz, J.-M.; Gobin, R.; Kirilovsky, D.; Rutherford, A. W.; Sugiura, M. *J. Biol. Chem.* **2004**, 279, 22809.
- (24) (a) Glass, R. S. *Top. Curr. Chem.* **1999**, 205, 1. (b) Li, Z.; Kutateladze, A. G. *J. Org. Chem.* **2003**, 68, 8236. (c) Wang, Y.; Shi, S.; Zhu, D.; Yin, G. *Dalton Trans.* **2012**, 41, 2612.

- (25) Yin, G.; McCormick, J. M.; Buchalova, M.; Danby, A. M.; Rodgers, K.; Day, V. W.; Smith, K.; Perkins, C. M.; Kitko, D.; Carter, J. D.; Scheper, W. M.; Busch, D. H. *Inorg. Chem.* **2006**, *45*, 8052.
- (26) Pal, S.; Chan, M. K.; Armstrong, W. H. *J. Am. Chem. Soc.* **1992**, *114*, 6398.
- (27) Goldsmith, C. R.; Cole, A. P.; Stack, T. D. P. *J. Am. Chem. Soc.* **2005**, *127*, 9904.
- (28) Gupta, R.; MacBeth, C. E.; Young, V. G., Jr.; Borovik, A. S. *J. Am. Chem. Soc.* **2002**, *124*, 1136.
- (29) (a) Quee-Smith, V. C.; Delpizzo, L.; Jureller, S. H.; Kerschner, J. L.; Hage, R. *Inorg. Chem.* **1996**, *35*, 6461. (b) Fallis, I. A.; Farrugia, L. J.; Macdonald, N. M.; Peacock, R. D. *J. Chem. Soc., Dalton Trans.* **1993**, 2759. (c) Kessissoglou, D. P.; Li, X.; Butler, W. M.; Pecoraro, V. L. *Inorg. Chem.* **1987**, *26*, 2487. (d) Chan, M. K.; Armstrong, W. H. *Inorg. Chem.* **1989**, *28*, 3777. (e) Chandra, S. K.; Chakravorty, A. *Inorg. Chem.* **1992**, *31*, 760.